ELECTRICAL RESISTIVITY AND HALL EFFECT OF
CUPROUS SULFIDE AND BISMUTH TELLURIDE
IN THE TEMPERATURE RANGE FROM
290°K TO 670°K

P. W. ERICKSON

ELECTRICAL RESISTIVITY AND HALL EFFECT

OF CUPROUS SULFIDE AND BISMUTH TELLURIDE IN THE TEMPERATURE

RANGE FROM 290°K TO 670°K

by

P. W. Erickson

Lieutenant Commander, United States Navy

Submitted in partial fulfillment of
the requirements for the degree of

MASTER OF SCIENCE

IN

MECHANICAL ENGINEERING

United States Naval Postgraduate School
Monterey, California

1 9 6 1

ELECTRICAL RESISTIVITY AND HALL EFFECT

OF CUPROUS SULFIDE AND BISMUTH TELLURIDE IN THE TEMPERATURE

RANGE FROM 290°K TO 670°K

by

P. W. Erickson

This work is accepted as fulfilling

the thesis requirements for the degree of

MASTER OF SCIENCE

IN

MECHANICAL ENGINEERING

from the

United States Naval Postgraduate School

ABSTRACT

An instrumentation and experimental technique for the measure-
ments of electrical resistivity and the Hall effect at elevated tempera-
tures is described. These two temperature-dependent properties are
uniquely determined for non-isothermal conditions and thereby are evalua-
tions at computed average temperatures within the specimens. The re-
sults of this investigation of cuprous sulfide and bismuth telluride in
the temperature range from 290°K to 670°K are presented and compared
with known published data. Resistivities are determined from measure-
ments of potential differences between selected points along the current
path through the specimens, while Hall effects are presented in terms
of the Hall coefficient, R_H, evaluated by Hall's equation, $V_H = R_H \dfrac{IH}{d}$.

Both cuprous sulfide and bismuth telluride show resistivities on
the order of 10^{-3} ohm centimeters, characteristic of semiconductor
materials, while the Hall coefficient for cuprous sulfide is estab-
lished at values less than 0.179 cubic centimeters per coulomb, and
the Hall coefficient for bismuth telluride decreases continuously with
increasing temperature from about 0.5 cubic centimeters per coulomb.

The instrumentation and investigation was conducted at the U. S.
Naval Postgraduate School, Monterey, California, during the winter and
spring of 1961.

ACKNOWLEDGEMENTS

TABLE OF CONTENTS

1. Introduction

For any homogeneous conducting material of constant cross-section, whose ends are equipotential surfaces, and in which the cross-sectional dimensions are small in comparison with the length of the conductor, the resistance to the flow of a continuous and uniformly distributed electrical current is expressed as

$$R = \rho \frac{L}{A} \tag{1A}$$

and conductance as

$$G = \frac{1}{\rho} \frac{A}{L} = \sigma \frac{A}{L} \tag{1B}$$

where
- R = electrical resistance
- L = length of the conductor
- A = cross-sectional area
- ρ = resistivity
- G = electrical conductance
- σ = conductivity

Metals are characterized by their high electrical conductivities; that is, they transmit large electrical currents under the influence of small differences in potential due to the presence of free electrons. The resistivity of metals also depends on the temperature, being roughly proportional to the absolute temperature, and increases with increase in impurity content. Whereas it is characteristic of metals that resistance increases with increasing temperature and with decreasing purity, a class of substance exists, both in crystalline and non-crystalline forms, for which the opposite is the case. This class is known as

1

semiconductors, in which conductivity increases with temperature in accordance with an exponential law of the form

$$\sigma = \sigma_c \, \epsilon^{\left(-\frac{\alpha}{T}\right)}$$

(2)

where σ_c and α are constants.

No exact demarcation exists between the resistivity of metals and semiconductors, and semiconductors and insulators - a third class of materials. J. N. Shive [10] [1] states 10^{-3} ohm centimeters and 10^{10} ohm centimeters, respectively, as delineating values between the three general classes of materials. Those materials possessing semiconducting properties, with resistivities in the somewhat arbitrary range of 10^{-3} ohm centimeters to 10^{10} ohm centimeters, are being examined with special and renewed interest toward improved thermoelectric power production on an economical basis. Basic properties required for one such evaluation of thermoelectric materials are:

the Seebeck coefficient (or thermoelectric power), S ,

the specific electrical resistivity, ρ , and

the specific thermal conductivity, K .

These three quantities are all functions of temperature and are combined to form a "figure of merit", Z , as follows:

$$Z = \frac{S^2}{\rho K}$$

(3)

The "figure of merit" has no intrinsic value but does afford means by which approximate comparisons of materials can be made. Clearly, materials of lower resistivity tend to produce a higher "figure of merit".

[1]Number in brackets designate references to Bibliography.

2

A maximum efficiency of power delivery of the special thermoelement circuity for Peltier heating and cooling, as described by Ioffe [6], is achieved for a maximum value of Z.

Another application of resistivity data is disclosed by the fundamental equation:

$$\sigma = m e \mu \qquad (4A)$$

where
σ = electrical conductivity

m = number of charge carriers

e = charge of the carrier

μ = mobility of the carriers

This simplified equation presupposes that the type of current carrier is either electrons or "holes". In essence, the expression predicts the conductivity as a function of the number of electrons or "holes" per unit volume, the charge of the electron (or "hole"), and the ease of movement of the electrons (or "holes") in an electric field. In the event that both types of carriers are present in a material and both contribute to conductivity, the total effect is the sum of the individual contributions as explicitly shown by equation (4A) above. Thus,

$$\sigma_T = m^- |e| \mu^- + m^+ |e| \mu^+ \qquad (4B)$$

where
σ_T = total electrical conductivity

m^- = number of electron carriers

m^+ = number of "hole" carriers

$|e|$ = absolute charge

μ^- = mobility of electrons

μ^+ = mobility of "holes".

This mixed type of conductivity is not commonly found in semiconductors but does appear in some metals.

3

Electrical conductivity data coupled with mobility evaluations
readily permit calculations of the concentration of carriers of semi-
conducting materials. However, conductivity is dependent not only on
the two aforementioned carrier types, but also on a third mode of charge
transport which is an inherent property of some materials. Conduction of
the electronic type, just described, dominates in most materials, but in
some, ionic conduction, or conduction by atomic imperfections, predomin-
ates. This mode is the transport or drift of charged ions under the in-
fluence of an electric field - not unlike conduction in a liquid electro-
lyte. Hannay [3] states that in some substances ion carrier densities
are intrinsically high - on the order of 10^{22} ions per cubic centimeter,
where, for comparison, densities of electronic carriers in bismuth tel-
luride are on the order of 10^{19} carriers per cubic centimeter. Further,
ionic conductivity can be expressed in the same parameters as electronic
conductivity in equation (4A).

Mobility is defined as the statistical average drift velocity which
a carrier acquires in the direction of an electric field of one volt per
centimeter [3,10] . The actual path of a particle carrier is not a
straight line but random and jerky, characterized by Brownian movement,
caused by collisions with other particles of the atomic lattice, and
other foreign particles of the nature of impurities and inclusions.
Of necessity, a specific value for mobility must be a statistical average
of many particles having various mean free path lengths and various ther-
mal kinetic energies. Specifically, mobility is directly proportional to
the length of the mean free path and inversely proportional to the square
root of the absolute temperature. [10]

4

It should be pointed out that two types of carrier mobility exist and are distinguished by the terms "Hall mobility", and "drift mobility" which is "conductivity mobility". As Shive [10] well describes, and is quoted:

> In such cases the particles being measured by the time-transient drift mobility method are believed to spend a significant fraction of their time in localized trapping centers in the crystal lattice. According to this picture, a carrier particle is locally attached to such a trap for a random interval of time. At the end of this interval it is released into the current stream where it executes a number of free paths, making a number of collisions, and drifts along for a short distance in the electric field. Sooner or later the particle becomes trapped by another trapping center farther on, then it is released again, etc. The particle is thus free to drift in the field only during random intervals of trappings. The mobility measured under these circumstances will naturally be lower than the 'true' mobility of the particle when it is free. On the other hand, the Hall mobility gives the mobility of the free particles on the fly.

"Hall mobility" evolved from original work in 1879 by E. H. Hall who discovered that, in some materials, a measurable potential difference appeared normal both to the direction of current flow and to the direction of a magnetic field. More precisely, if a current is flowing longitudinally through a material specimen in the X direction (Fig. 1) and is within a magnetic field in the Y direction, a potential gradient will appear transversely in the Z direction. The Hall voltage equality follows as

$$V_H = R_H \frac{IH}{d}$$

(5)

where V_H = Hall voltage

I = electric current

H = magnetic field

d = thickness of material

5

The magnitude of the Hall voltage as measured at the surface of the specimen is directly proportional to the magnitudes of both the current
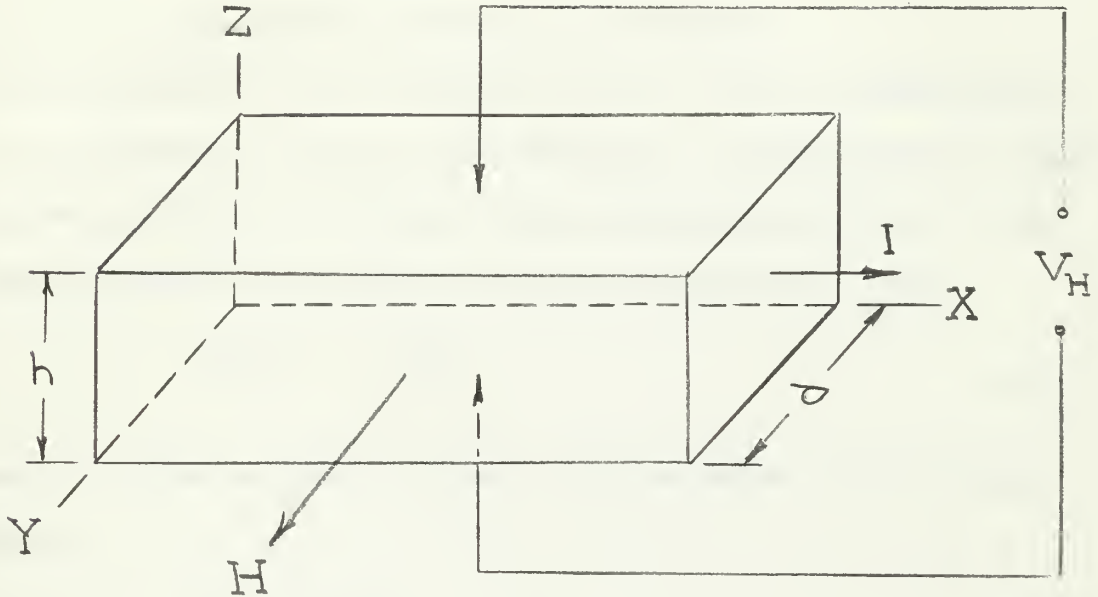
Fig. 1 Hall effect

and the magnetic field and inversely proportional to the specimen dimension in the direction of the magnetic flux. Experimental data for these parameters permit evaluation of the Hall coefficient, R_H.

Hall mobility, as a function of electrical conductivity and the Hall coefficient, results in the expression

$$\mu_H = \sigma R_H \tag{6}$$

A relationship between the Hall coefficient and the carrier concentration may be established in the following way. Electric current defines an electric charge in motion. The rate at which a quantity of electricity flows past a given point in a circuit determines the magnitude of the current, that is, (refer Fig. 1 above).

6

$$I = meuhd \tag{7}$$

where u = average drift velocity in X direction

h = cross-section dimension in Y direction

d = cross-section dimension in Z direction

In the examination of the balance of forces to which a charged particle is subjected, at steady state conditions, the Hall potential resulting from the build-up of charge at the surfaces must be equal to the magnetic force in the direction of the Hall potential. Thus,

$$\frac{euH}{c} = \frac{eV_H}{h} \tag{8}$$

where c is the velocity of light. The combination of (7) and (8) produces

$$V_H = \frac{IH}{cmed} \tag{9}$$

A comparison of (9) and (5) discloses that

$$R_H = \frac{1}{cme} \tag{10A}$$

which establishes the relation between the Hall coefficient and the carrier concentration. Of course R_H will assume a negative or positive value depending upon the sign of the charge. It should be understood that R_H varies with temperature because of the temperature dependence of the carrier concentration.

R_H, as evaluated by Hall's voltage equation (5), is based on a uniform drift velocity of carriers, a long-time average of instantaneous values superimposed on random thermal motions. Equation (10A) is modified

7

to account for the averaging of the actual drift velocity over all such thermal velocities, as follows,

$$R_H = \frac{3\pi}{8cm e} \qquad \text{(10B)}$$

The modified Hall coefficient is derived by Seitz [9] .

8

2. Instrumentation and Experimental Method

Because electrical conductivity and the Hall coefficient are essential to the evaluation of carrier mobility in the manner previously described, good experimental procedure dictates that pertinent and necessary data be taken <u>simultaneously</u> over the range of temperatures for which properties are desired, for the following reasons:

(a) "aging" of the specimen (loss of current carriers with time)

(b) heat treatment effects

(c) change in impurity concentrations

(d) oxidation at prolonged elevated temperatures

(e) structural changes

This concept forms a basis of instrumentation.

Published works dealing with earlier investigations of resistivity and Hall effect at elevated temperatures report the use of small electric furnaces of non-ferromagnetic materials for temperature control. The more modern equipment incorporates an electromagnet built into a specially constructed oven. The present study employed a simple radiant-type heater unit of 28 gage Nicrome wire wound non-inductively along a short length of slotted Vicor tubing (See Fig. 3, page 11.)

Temperature determinations (see Appendix II) were deduced from three thermocouple readings taken at the ends and midpoint of the specimens.

The specimen was held firmly in position at the ends by two pairs of wafer-like discs, machined and formed from Lava block, chemically anhydrous aluminum silicate, fired to 2000°F after fabrication. The outermost discs were drilled for insulated thermocouple (and current) leads, while the inner ones were recessed to hold the copper strip electrodes,

9

THERMOCOUPLE
INSULATOR

ELECTRODE

THERMO-
COUPLE
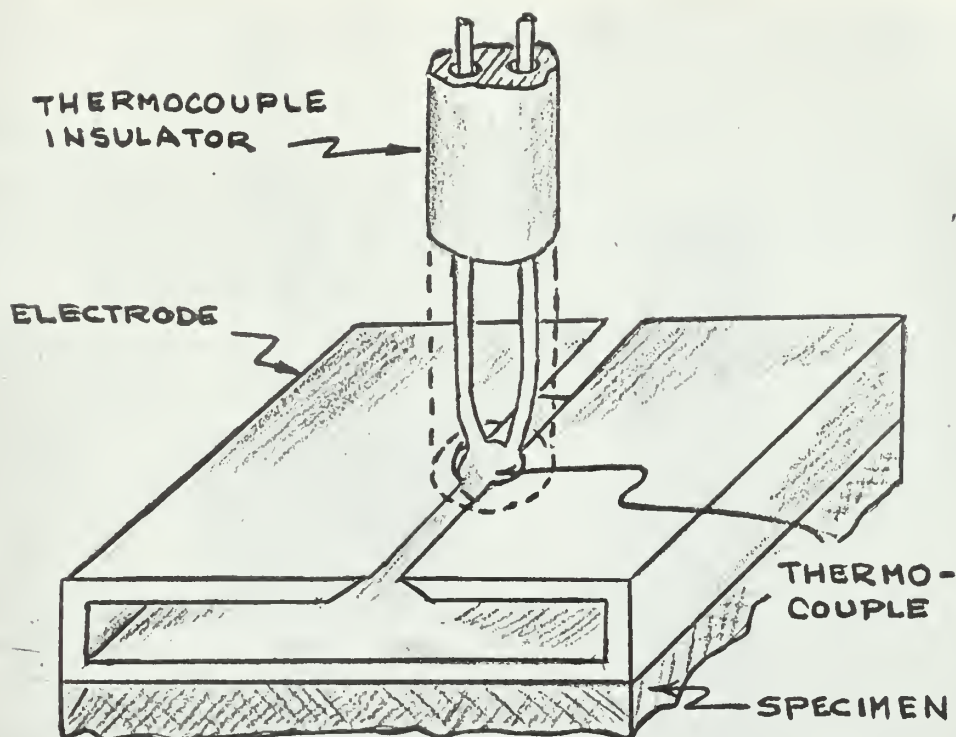
SPECIMEN

Fig. 2 Sketch of Copper Electrode with Thermocouple

whose configuration is sketched in Fig. 2. The contact area of the
electrodes was equivalent to the cross-section of the specimens to in-
sure a uniform current density through the specimen. No bonding sub-
stance was used between the electrodes and the specimen. The disc pairs
were drilled and wired together and, under the compressive force of two
diametrically opposed tungsten springs, formed the specimen holder as
shown in Figs. 3 and 4, pages 11 and 12. Additionally, the discs were
drilled to accommodate the heater leads, probe leads, and two glass
aligning rods, all which passed into and through a rubber stopper. This
entire assembly was inserted into a cylindrical pyrex glass container,
sealed off at the bottom end and provided with two vacuum stop-cocks
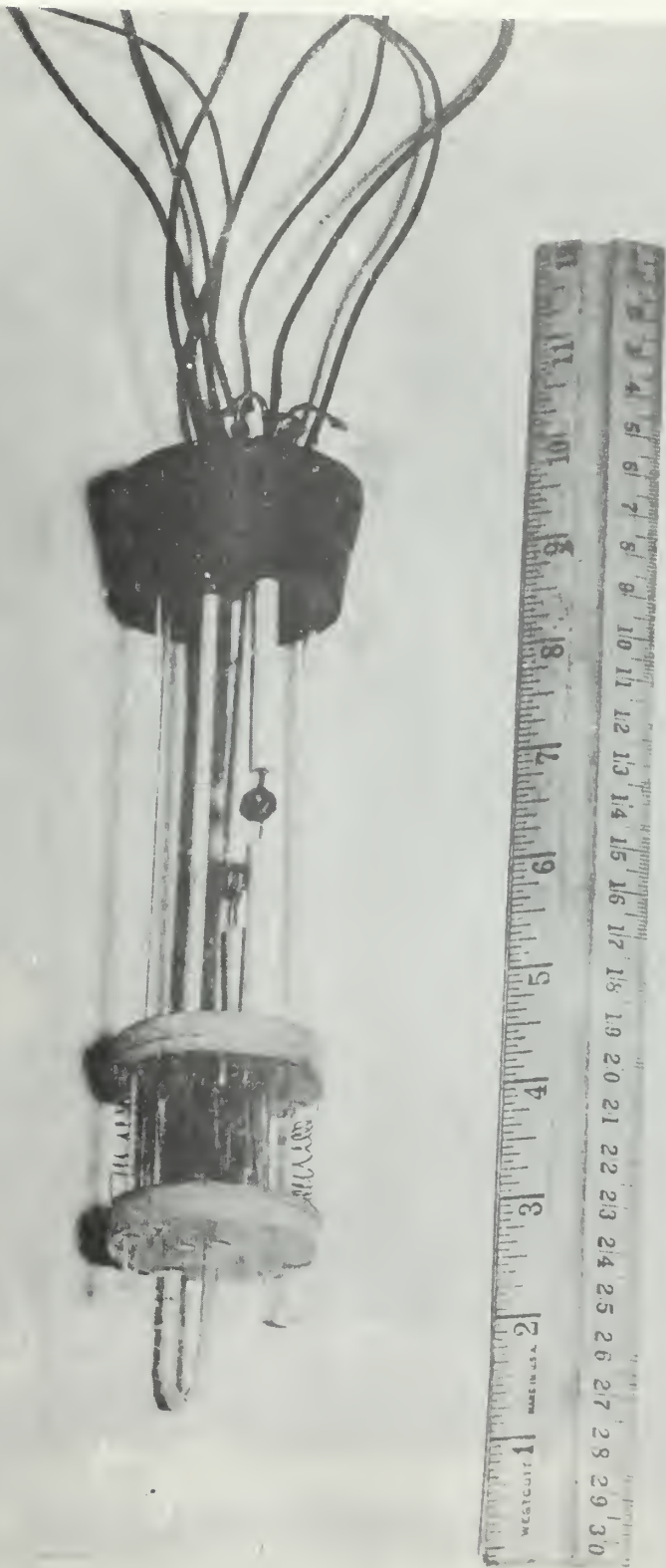
Fig. 3 Specimen Holder Assembly

FIG. Lower probe holder and heater removed.
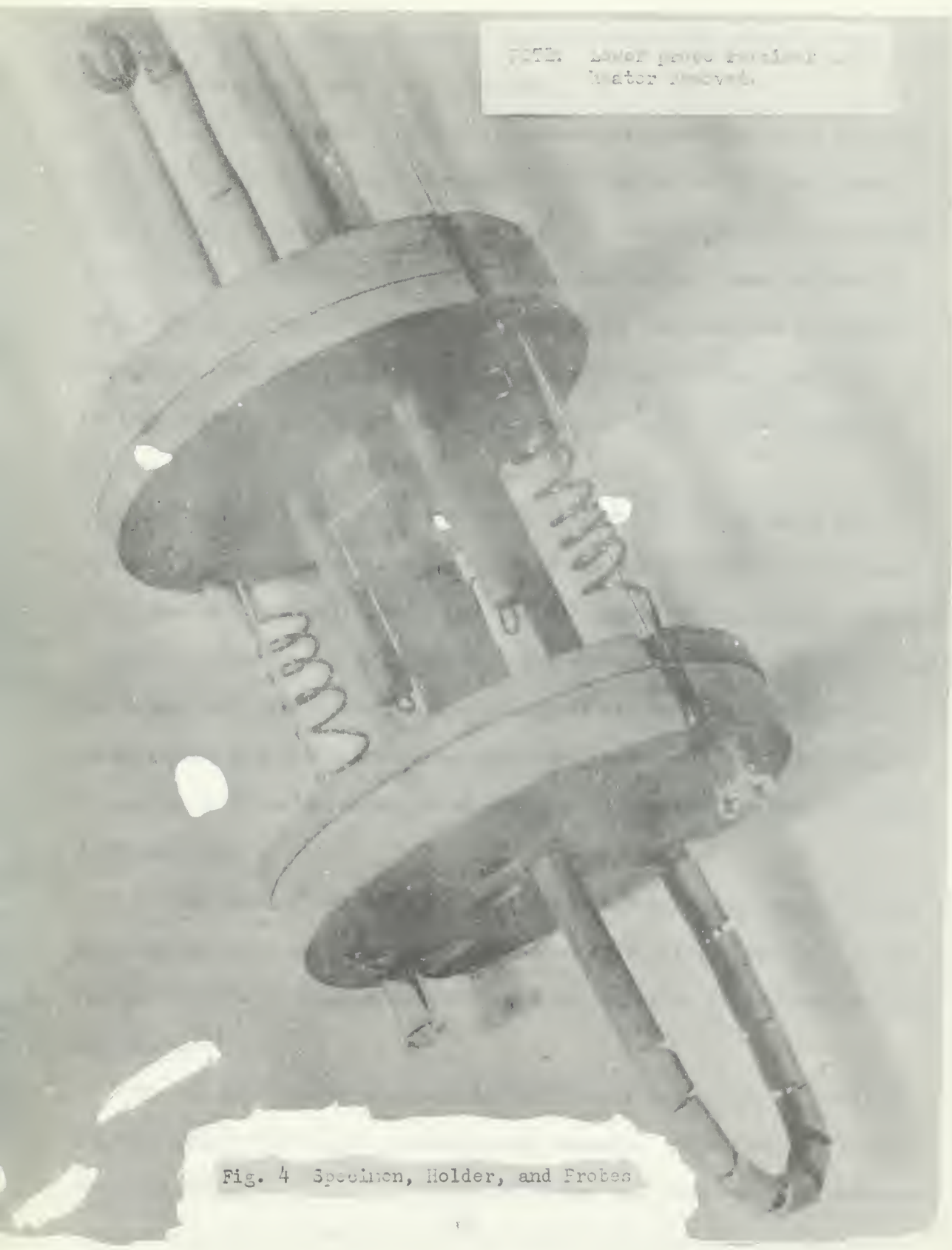
Fig. 4 Specimen, Holder, and Probes

for drawing and releasing vacuum. Sealing was accomplished by wax, Glyptal, and type N stop-cock lubricant.

Two platinum-platinum and 10% rhodium thermocouples, also serving as current conductors, were attached to the copper strip electrodes by pressure fit in the manner shown in Fig. 2. The two pairs of tungsten probes, shaped under heat and pointed by acid attack, were adjustable from a point above the stopper and external to the specimen container. The probes were held in contact with the specimen through their own spring property, and were kept aligned by two small slotted glass retainers fitted to the specimen.

All voltage lead connections were immersed in an ice bath (0°C), agitated by a motor-driven stirrer. Voltage measurements were accomplished by the standard null method using a K-2 potentiometer and Rubicon galvanometer. The four probes located in pairs approximately one-third and two thirds the distance along the length of the specimen facilitated simultaneous and duplicate measurements of resistance and Hall voltage, by toggle selector switching schematically illustrated in Fig. 5 on the following page.

Adjustments of current from a standard six volt storage battery were made through a decade resistance box and a slide wire rheostat. Direct current for the K-2 potentiometer was from two cells of another six volt storage battery.

The magnetic field was provided by a water-cooled Varian electromagnet, Model V-4007, with conical pole inserts. Excessive heating of the pole faces was prevented by wrapping the specimen container externally with a layer of aluminum foil and several layers of asbestos paper.

13
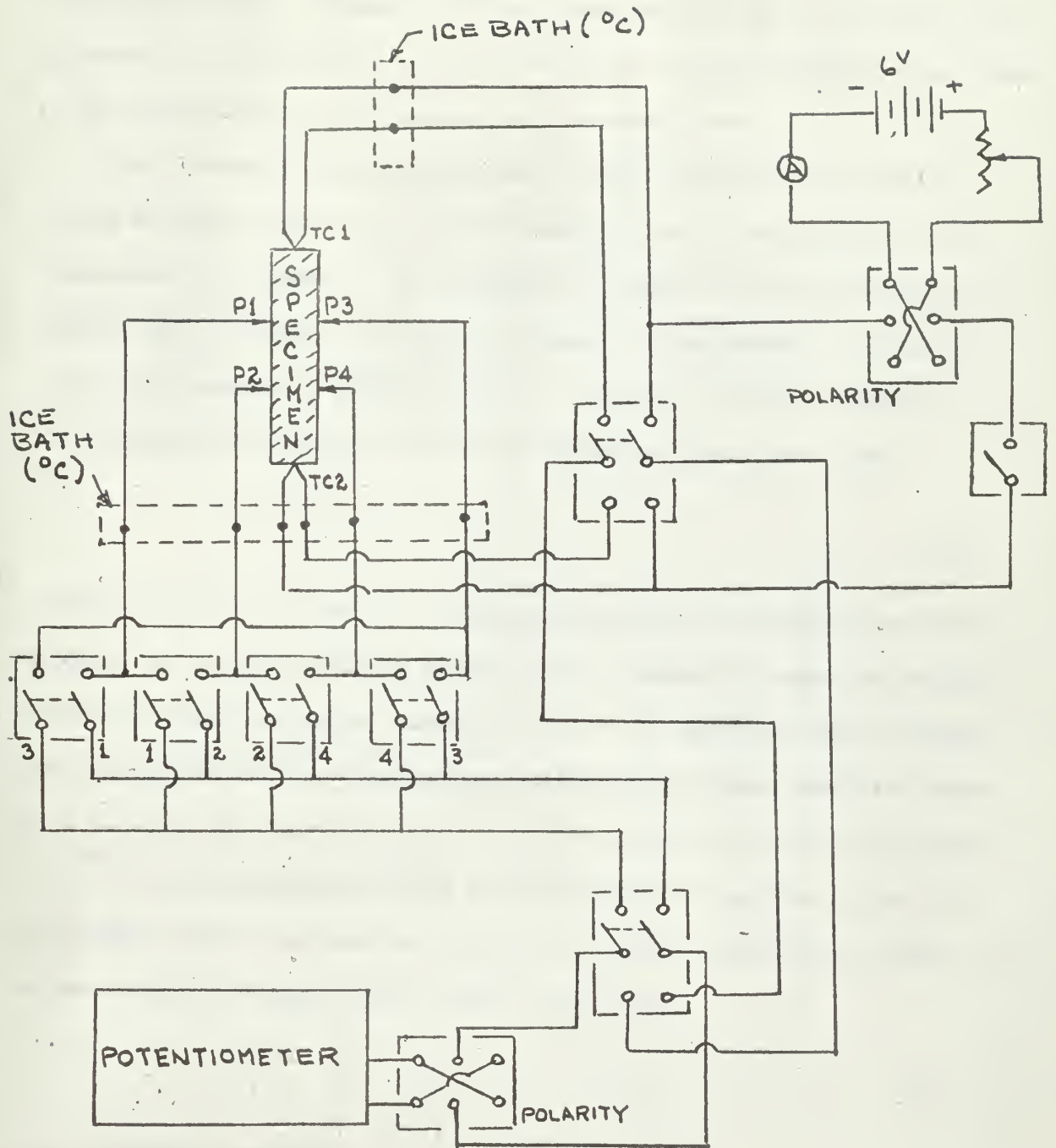
Fig. 5 Schematic of Wiring and Switching Arrangement

14

Voltage readings were taken only after temperature checks indicated that thermodynamic conditions had reached steady state. For resistivity measurements, currents of 50 milliamperes and 100 milliamperes were selected as most suitable, and for Hall effect 100 milliamperes was found to be appropriate, for reasons to be discussed later.

Both current reversal and magnetic field reversal are normally necessary to account for all first order galvanic, thermomagnetic, and thermoelectric effects.[2] As Lindberg [8] points out, opposite probes to measure Hall voltage, if perfectly aligned on equipotential planes at no field, will measure a voltage which is the sum of the Hall potential and the thermocouple potential due to Ettinghausen effect such that

$$V = V_H + V_E \tag{11}$$

Since the Hall effect and the Ettinghausen effect are both current dependent, it is impossible to evaluate each separately under the circumstances. Lindberg states, however, that in the specific case of germanium, investigations have shown that Ettinghausen effect comprises about five percent of the total and is usually neglected in the evaluations.

Peltier heating and cooling at the points of juncture of the current leads and of the specimen initiate a thermal current that brings into the Nernst and Righi-Leduc effects such that

$$V_1 = +V_H + V_E + V_N + V_{RL} \tag{12}$$

and by current reversal,

[2] Refer to Glossary, Appendix VI, for definitions of effects later mentioned.

$$V_2 = -V_H - V_E + V_N + V_{RL} \tag{13}$$

Since both the Nernst and the Righi-Leduc effects are current indepen-
dent, these potentials can be eliminated by current reversals and combina-
tion of equations (12) and (13).

Another first order effect is the IR drop possible due to probe
misalignment, but, if by design the opposite probes are adjustable for
zero potential, the need for magnetic field reversal in addition to cur-
rent reversal is essentially eliminated. However, the conventional prc-
cedure entails both current and field reversals resulting in four vol-
tage measurements, V_1, V_2, V_3, and V_4:

For H^+ and I^+,

$$V_1 = +V_H + V_E + V_N + V_{RL} + V_{IR} \tag{14}$$

for H^+ and I^-,

$$V_2 = -V_H - V_E + V_N + V_{RL} - V_{IR} \tag{15}$$

for H^- and I^-,

$$V_3 = +V_H + V_E - V_N - V_{RL} - V_{IR} \tag{16}$$

and for H^- and I^+

$$V_4 = -V_H - V_E - V_N - V_{RL} + V_{IR} \tag{17}$$

It follows that

$$V_H + V_E = \frac{V_1 - V_2 + V_3 - V_4}{4} \tag{18}$$

Departure from the conventional procedure was necessary because of the
inability to reverse the magnetic field, and hence adjustable probes be-
came not only desirable but mandatory.

This basic technique as described was extensively modified in the
present investigation of cuprous sulfide and bismuth telluride. For

16

Hall voltage measurements, ample time was allowed for thermal energy transfer to reach steady state as indicated by thermocouple readings. With direct current flow, Peltier and Thomson effects prevail to some small degree. With essentially zero magnetic field,

$$V_1 = V_{TC} \tag{19}$$

where V_{TC}, is the net thermocouple effect in the probe-specimen-probe circuit in the absence of magnetic influence. With the magnetic field energized, a second voltage reading, V_2, would include some contributions from Ettinghausen[3], Ettinghausen-Nernst, Righi-Leduc, Nernst, and Hall effects, which may be expressed as

$$V_2 = V_E + V_{E-N} + V_{RL} + V_N + V_H + V_{TC} \tag{20A}$$

An expeditious second reading minimizes Ettinghausen, Righi-Leduc, and Nernst effects because of the time requirement for thermal gradients to form. With the probe pairs located symmetrically in the central portion of the specimen, the thermal current density will consequently be small and the transverse electric field produced by the Ettinghausen-Nernst effect can be neglected. Then equation (20A) is simplified to

$$V_2 = V_H + V_{TC} \tag{20B}$$

and combining equations (19) and (20B),

$$V_H = V_2 - V_1 \tag{21}$$

Current reversal, therefore, provided no effective cancellation of undesired components of readings in the Hall effect procedure except to verify and average data, and disclose any anisotropy of the specimens.

It is imperative, particularly for small Hall voltages, that consecutive readings, V_1 and V_2, be made as rapidly as possible, for a

[3] Refer to footnote 2, page 15.

slow and continuous drift in V_{TC} will prevail due to the changing See-
beck effect in the probe-specimen circuitry with ionic motion, impurity
changes, and some unavoidable temperature variance. Elapsed time must
be kept at a minimum to produce reliable evaluations.

Only one of the associated effects just considered plays an apprec-
iable part in the resistivity measurement technique were effective cancel-
lation of thermocouple effect is desired to produce the resultant IR drop.
As the data indicates (Appendix IV), the thermocouple effect, V_{TC}, can
be appreciable and dominating over small IR drops. Current reversal ac-
companied by rapid consecutive readings results in two simple equations,

$$V^+ = V_{IR} + V_{TC} \tag{22}$$

and

$$V^- = -V_{IR} + V_{TC} \tag{23}$$

Then,

$$V_{IR} = \frac{(V^+) - (V^-)}{2} \tag{24}$$

The general physical arrangement of apparatus is depicted in the
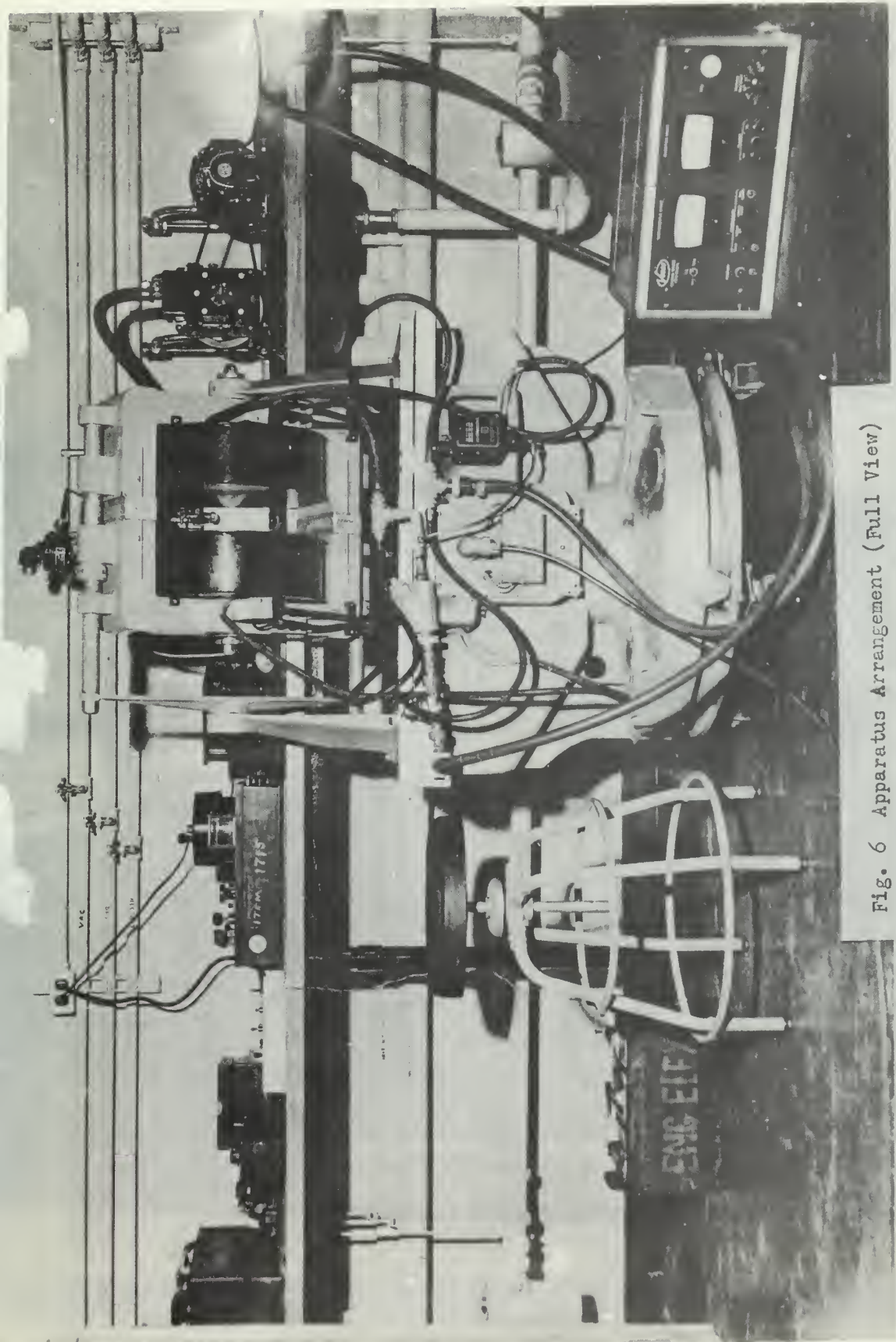form of photographs, Figs. 6 and 7 on the following two pages.

Fig. 6 Apparatus Arrangement (Full View)
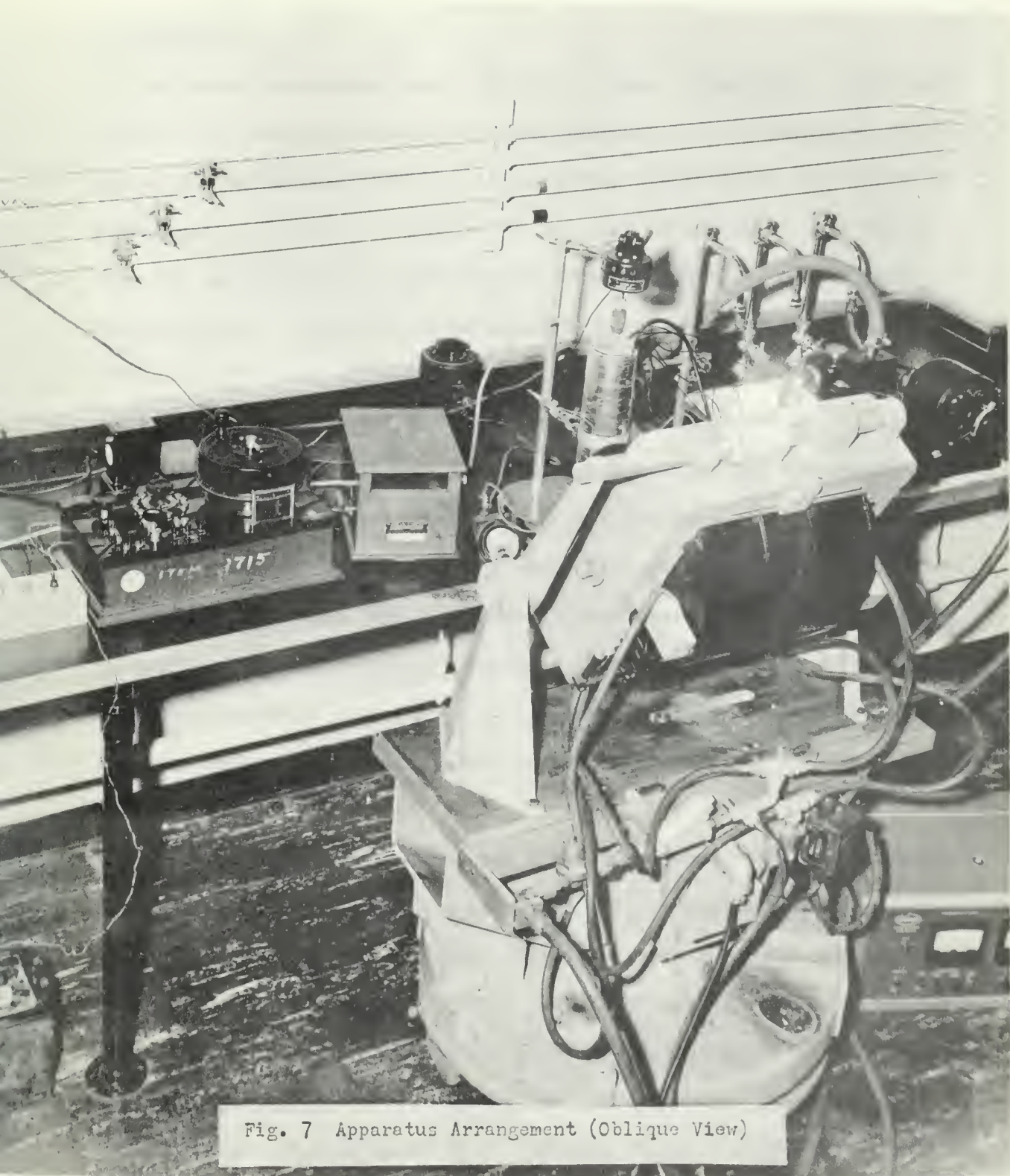
Fig. 7 Apparatus Arrangement (Oblique View)

3. Results

At each temperature level within the range of interest, resistance and Hall voltage measurements were made pursuant to the technique described in the previous section. Concurrent data required the switching arrangement and circuitry previously referred to in Fig. 5, and the design was satisfactory for the purpose intended. The values for resistivities and Hall coefficients evolved from equations (1A) and (5), respectively.

Fig. 8, page 24, displays the temperature dependence of the resistivity of cuprous sulfide, and Fig. 9, page 26, shows the temperature dependence of resistivity of bismuth telluride. Fig. 10, page 27, presents the Hall coefficient of bismuth telluride as a function of temperature. Some comparisons are afforded by curves constructed from published data as reproduced in Appendix I. Direct comparison of the cuprous sulfide resistivity curves is illogical in view of the noted differences in the percentages of excess sulfur in the various specimens separately investigated.

For all temperatures examined, the Hall voltage produced in cuprous sulfide was less than one microvolt and not within the capability of the potentiometer to evaluate. Trial currents of magnitudes up to 1.5 amperes, corresponding to a current density of approximately six amperes per square centimeter, and reduced specimen thickness failed to produce Hall voltages of measurable magnitudes. Consequently, for a maximum field strength of 5700 gauss and a specimen current of 100 milliamperes, an upper limit of .179 cubic centimeters per coulomb (calculations in Appendix V) is established as a property of cuprous sulfide in the

21

temperature range from 290°K to 670°K.

Temperature determinations for resistivity were based on the average value between relevant probes, whereas the nature of Hall effect dictated the evaluation of average temperatures within the entire specimen (see Appendix V).

As noted in the data (Appendix IV), the magnetic field strength was recorded at 5700 gauss, measured by gaussmeter. This value corresponds to the maximum attainable for a pole gap of 4.60 centimeters and maximum rated coil current of 1.2 amperes. The electromagnet characteristic curves give an approximate gap field of 6400 gauss for a corresponding current and for cylindrical pole caps with a five centimeter gap. Some reduction in field strength must be attributed to the higher flux impedance at the surfaces of the six cadmium-plated spacer inserts required for appropriate gap adjustment.

TABULATED RESULTS

CUPROUS SULFIDE SPECIMEN

Average Temperature T degrees Kelvin	Average Electrical Resistivity $\tilde{\rho}$ ohm centimeters
294	3.68×10^{-3}
327	3.52
339	3.30
353	2.94
365	2.68
374	2.86
401	3.36
413	3.64
433	4.23
444	4.28
471	3.90
501	3.41
526	2.71
547	2.31
577	1.91
596	2.31
616	2.86
641	3.60
666	4.18

Hall coefficient $< 1.79 \times 10^{-1}$ cm^3 per coulomb throughout the entire temperature range from 294°K to 666°K.
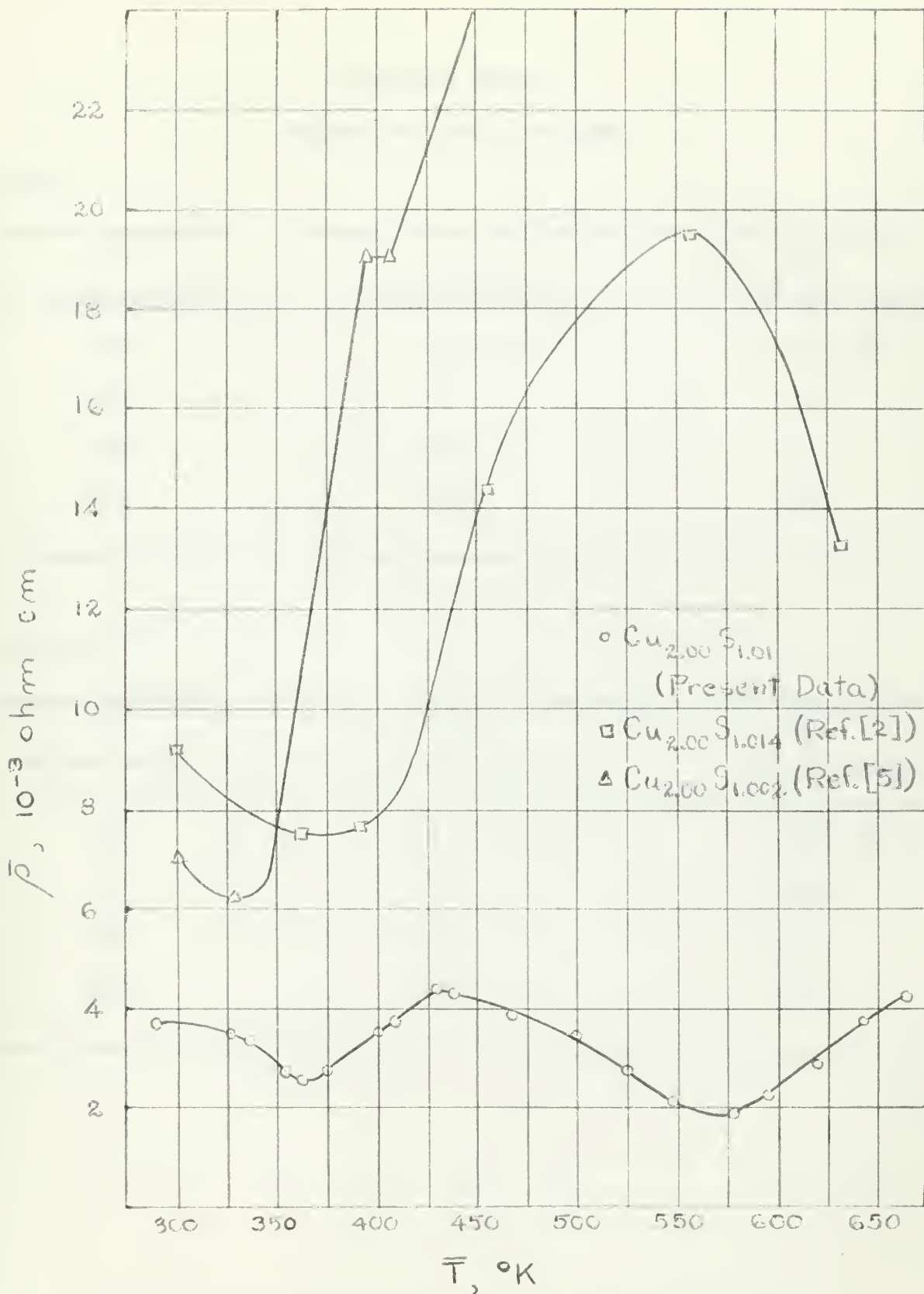
Fig. 8   Temperature Dependence of Electrical Resistivity

24

TABULATED RESULTS

BISMUTH TELLURIDE SPECIMEN

Probes 1 - 3:

Average Temperature $\overline{T}$ degrees Kelvin	Average Electrical Resistivity $\overline{\rho}$ ohm centimeters	Hall Coefficient R_H cm^3 per coulomb
294	1.40×10^{-3}	5.3×10^{-1}
370	1.71	5.3
485	1.46	3.1
633	1.14	1.8

Probes 2 - 4:

Average Temperature $\overline{T}$ degrees Kelvin	Average Electrical Resistivity $\overline{\rho}$ ohm centimeters	Hall Coefficient R_H cm^3 per coulomb
294	1.44×10^{-3}	3.9×10^{-1}
371	1.77	4.4
485	1.50	3.1
634	1.19	0.9

Fig. 9 Temperature Dependence of Electrical Resistivity
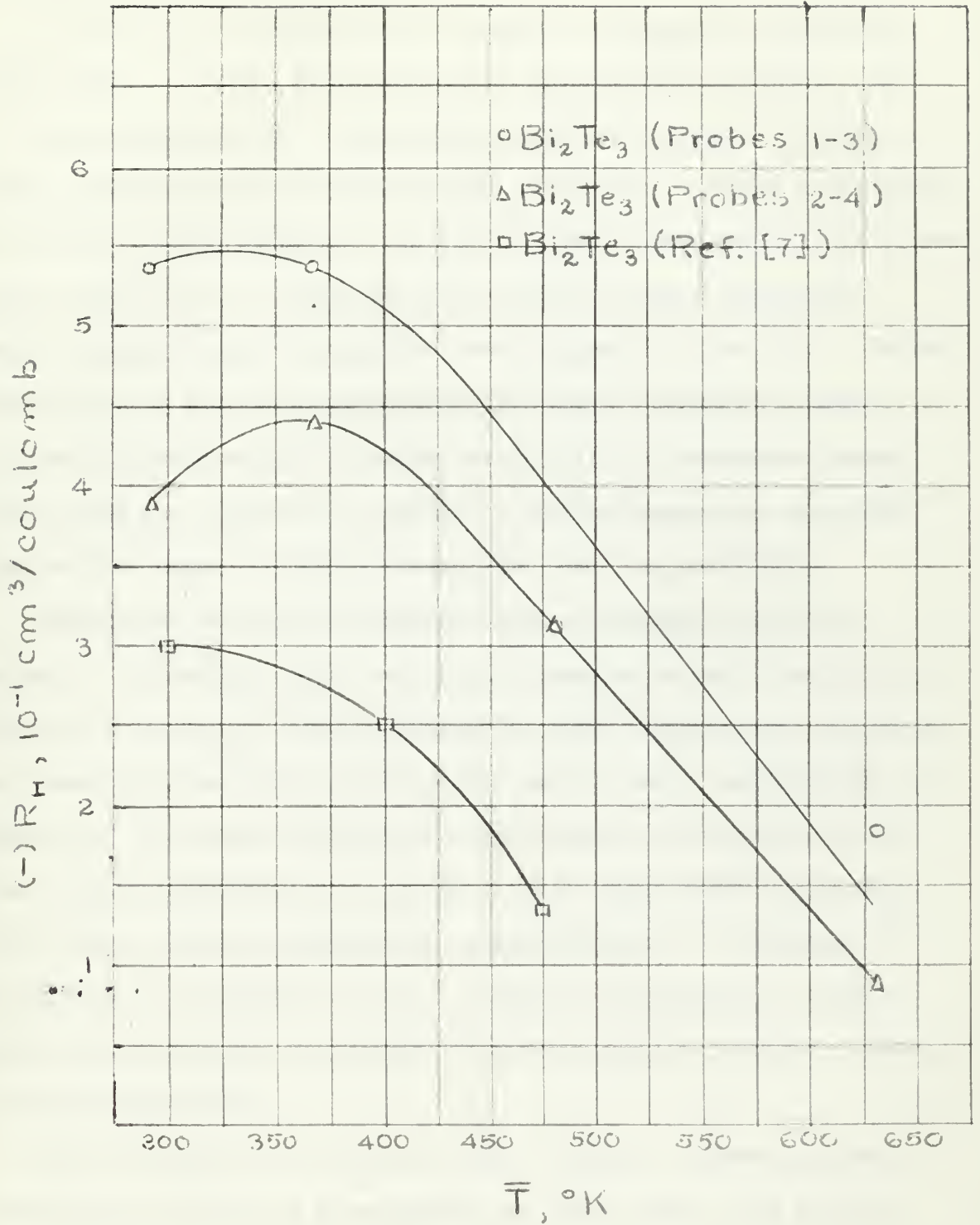
Fig. 10 Temperature Dependence of Hall Coefficient

4. Discussion of Results with Conclusions

E. Hirara [5] established three conduction phases for cuprous sul-
fide, namely, α-phase (above 470°C), β-phase (470°C to 110°C), and
γ-phase (below 110°C). He further states that in the γ-phase,
cuprous sulfide shows the characteristic properties of P-type semiconduct-
ors such as cuprous oxide [1] ; in the β-phase a phenomenal ionic current
appears; and in the α-phase the ionic current becomes negligible.
Numerous authors[4] have reported the lower temperature transition. In the
examinations of electrical conductivity of several samples of cuprous
sulfide of varying amounts of excess sulfur [5] the temperature depen-
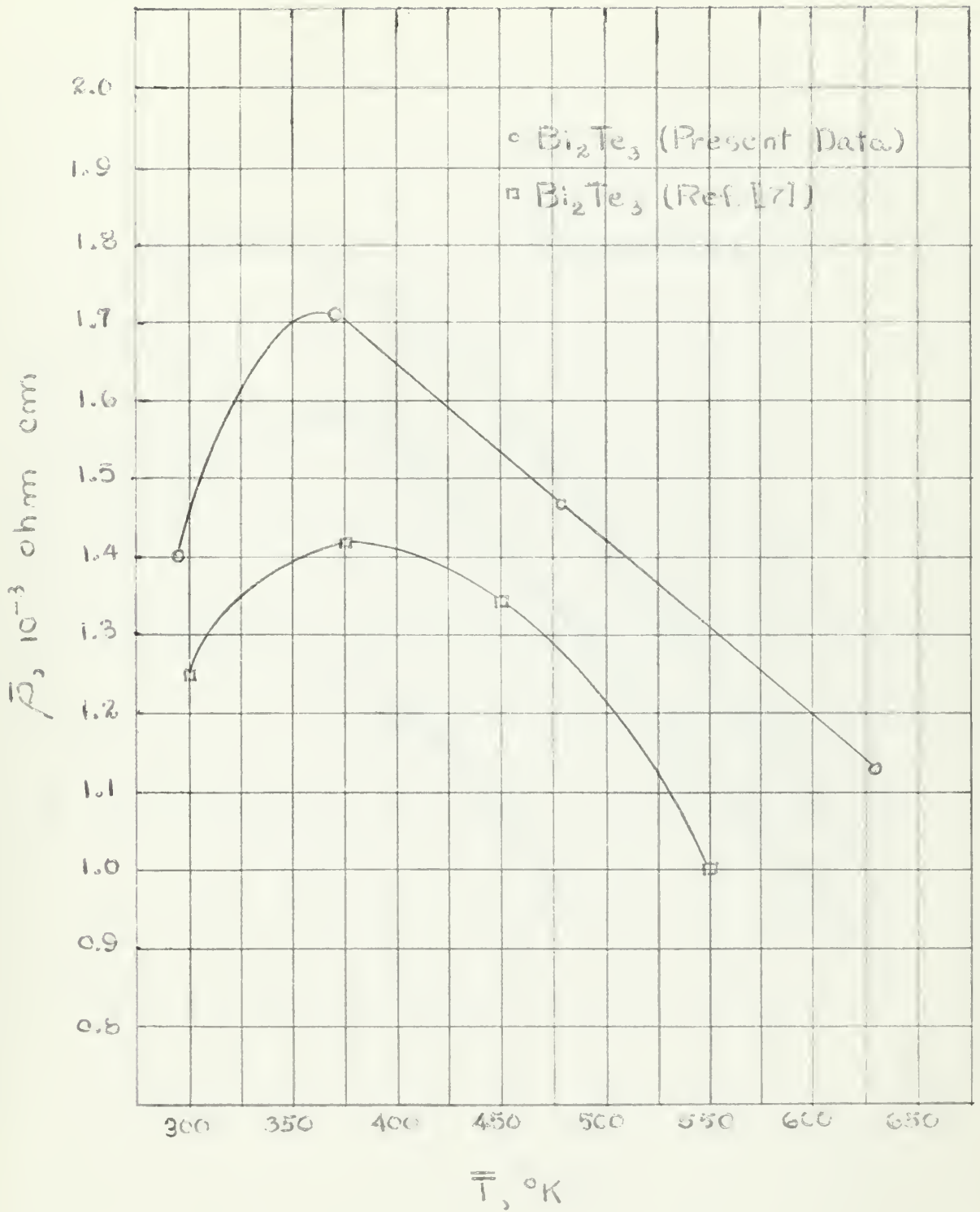dence curves are consistant in quality, but displacements in magnitude
indicate the larger the sulfur excess, the lower the resistivity.

The results of this investigation conform favorably in several
respects. The quality of the resistivity-temperature curve (see Fig. 8,
page 24) is similar to those publicized by other investigators, although
the transition temperature points do not exactly match, particularly the
higher one. The curve resulting from measurements decreases initially
from ambient temperature to a minimum value at about 365°K (92°C) which
is the lower transition temperature separating phase γ and phase β.
The decline in resistivity in the γ-phase is attributed to a longer
carrier mean free path, an increase in carrier mobility, and very likely
some ionic conduction.

As the temperature is raised in the β-phase, a sudden increase
in resistivity appears as a consequence of ionic motion. The periodic
field of the crystal lattices is disrupted and distorted to the extent

[4] E. A. Posnjak and H. E. Merwin, P. Rahlfs (1936), M. J. Buerger and
N. W. Buerger (1942, 1944).

28

of greatly reducing the mean free path length of carriers as well as reducing mobility. The rise of resistivity to a maximum value at about 540°K (267°C) exemplifies the phenomenal change in atomic characteristics. It will be observed that another minimum resistivity point is reached at a temperature of about 570°K (297°C) which establishes the transition point between the β-phase and the α-phase. As the temperature increases further in the α-phase, resistivity increases in the typical exponential manner to the melting point (see Fig. 12, page 36).

It can then be concluded that three phases of resistivity is a significant property of cuprous sulfide, that the transition points are temperature dependent and well-defined, and that the variations within each phase is explainable in terms of particle theory, mobilities, and carrier concentrations. Among several independent investigations, variations within an order of magnitude, or so, are due essentially to differences in element proportions or excesses, heat treatment effects on atomic structure, inevitable introduction of some impurities in handling and experimentation, and, of course, experimental error.

An examination of previous results [5] indicates that the maximum value of the Hall coefficient in the case of stoichiometric cuprous sulfide is on the order of 0.4 cubic centimeters per coulomb, decreasing appreciably and consistantly with increase in excess sulfur content to 0.1 cubic centimeters per coulomb in specimens of 0.2 percent excess. It can reasonably be expected, then, that cuprous sulfide of one percent excess sulfur would further reduce the Hall coefficient to such an extent that much more sensitive apparatus is required for evaluations. This fact offers an explanation why a Hall voltage was not observable.

29

It has been reported [7] that small deviations from stoichiometric composition of bismuth telluride have a large effect on its electrical conductivity. Also, the anisotropy of single crystal samples is depicted by the fact that conductivity was found to be about 1.5×10^3 ohm^{-1} centimeters^{-1} at ambient temperature parallel to the crystal layers and about 50 ohm^{-1} centimeters^{-1} perpendicular to the layers. The results of the present investigation show close conformity with published results in respect to the temperature dependence of resistivity and Hall effect of bismuth telluride (see Figs. 9 and 10, pages 26 and 27). Regard should be given to the handicap imposed by the relative insensitivity (one microvolt) of the measuring equipment, and reading errors are potentially large.

In reiteration of an important point, unavoidable temperature effects, rates of heating and cooling, time at temperature, stability of chemical combinations, etc., all will affect gross measurements of desired voltages. For this reason, results are non-repeatable in varying degrees of magnitude. Specifically, data accumulated by temperature reduction and temperature elevation cannot be superimposed. Time dependency is dramatically evident where ionic conduction occurs. The charged ions migrate to the ends of the specimens under the attracting force of a potential. When the potential is altered or removed, time is required for these particles to diffuse back to "equilibrium" positions in the atomic network.

One might conclude that a substance, such as cuprous sulfide or bismuth telluride, of moderately high thermoelectric power, i.e. large Seebeck effect, would have an appreciable Hall effect. Ioffe [6] points

out two relations which clarify this conception in the event that a
material has mixed conductivity - both electron and "hole" carriers:

$$S \propto \frac{m^+\mu^+ - m^-\mu^-}{m^+\mu^+ + m^-\mu^-} \qquad (25)$$

$$V_H \propto \frac{(\mu^+)^2 m^+ - (\mu^-)^2 m^-}{(\mu^+ m^+ + \mu^- m^-)^2} \qquad (26)$$

where S is the Seebeck coefficient, and other symbols are as previously
defined. Where only one type of carrier is in prominence, say "holes",
and neglecting any contribution from carriers of the opposite sign,

$$S \propto 1 \qquad (27)$$

and

$$V_H \propto \frac{1}{m^+} \qquad (28)$$

Inspection of these proportionalities indicates that a high "hole"
concentration will tend to reduce the Hall effect. Both cuprous sulfide
and bismuth telluride have Seebeck coefficients greater than 100 micro-
volts per degree centigrade and, as presented, relatively low Hall co-
efficients.

5. Problem Considerations and recommendations

One of the principal considerations involved in this experimental work is the introduction of impurities into the specimen for which the electrical properties of semiconductors have a great sensitivity. Some contamination is inevitable, and diffusion into the specimen proceeds at high rates at elevated temperatures. Compatibility of materials in contact with the sample should be determined to minimize chemical reaction, particularly at the elevated temperatures. It is very likely that some copper atoms did diffuse into the specimens from the electrodes to change the composition of the material. Some oxidation did occur, with a partial pressure existing within the container.

Probes composed of the same material as the specimen would be ideally suited to small voltage measurements in order to eliminate the thermocouple effect between dissimilar materials. Indeed, the net effect can override and obscure the desired voltage measurement of low value. Additionally, non-isothermal conditions at points of contact, due not only to Ettinghausen effect but to non-uniform heating, is prime consideration in the adoption of any technique.

Good thermal contact between thermocouples and points of temperature measurements is not a simple matter, while some contamination and cold working of thermocouples is unavoidable during installation and results in small deviations from standard conversion tables. Platinum - platinum plus ten per cent rhodium is suitable for precise temperature measurements from zero degrees centigrade upward to above 1000 degrees centigrade because of the inertness and stability of these materials at high temperature in oxidizing environments.

Flexibility in the design of an enclosure for the specimen is usually detrimental to good vacuum sealing. An alternative to a vacuum would be an inert gas envelope, if it were not for the disruptive effects of convection currents. Accessibility is essential for sample replacements and for adjustment of probes, when the design and technique require, and is another noteworthy problem.

By way of recommendation, experimenters should describe what heat treatments, if any, that a sample undergoes, for presenting a comprehensive and true evaluation of data on a specific material. Reports of separate investigations of a like material can be correlated to express some influence of heat treatment on properties, and such correlations then become an important source of information on a class of materials which may be potentially good thermoelements, or which may serve as a basic substance to be improved by "doping".

Admittedly, the non-isothermal technique in the foregoing investigation precludes optimum accuracy of results. However, such designs based on simplicity and flexibility permit, at the least, approximate and cursory evaluations of those discrete properties upon which the effectiveness of thermoelectric materials depends, as typified by the "figure of merit" relation.

6. Bibliography

1. Angello, S. J., Hall Effect and Conductivity of Cuprous Oxide, Physical Review, Vol. 62, Oct. 1 and 16, 1942.

2. Davisson, J. W. & Pasternak, J., Status Report on Thermo-electricity, NRL Memorandum Report 1037, U. S. Naval Research Laboratory, Wash., D. C., Mar. 1960.

3. Hannay, N. B., Semiconductors, New York, Reinhold Publishing Corp., 1959.

4. Hirahara, E., The Physical Properties of Cuprous Sulfides-Semiconductors, Journal of the Physical Society of Japan, Vol. 6, No. 6, pp. 422-427, Nov-Dec. 1951.

5. Hirahara, E., The Electrical Conductivity and Isothermal Hall Effect in Cuprous Sulfide, Semi-Conductor, Journal of the Physical Society of Japan, Vol. 6, No. 6, pp. 428-437, Nov.-Dec. 1951.

6. Ioffe, A. F., Semiconductor Thermoelements and Thermoelectric Cooling, London, 1957.

7. Konorov, P. P. (A. A. Zhdanov State University, Leningrad), Electrical Properties of Bismuth Telluride, Zhur. Tekh. Fiz. Vol. 26, pp. 1400-1405, 1956.

8. Lindberg, O., Hall Effect, Proceedings of the Institute of Radio Engineers, Vol. 40, No. 11, pp. 1414-1419, Nov. 1952.

9. Seitz, F., The Modern Theory of Solids, McGraw-Hill Book Co., Inc., New York and London, 1940.

10. Shive, J. N. Semiconductor Devices, New York, D. Van Nostrand Co., Inc. 1959.

11. Stauss, H. E., Status Report On Thermoelectricity, NRL Memorandum Report 969, U. S. Naval Research Laboratory, Wash., D. C., Dec. 1959.

MATERIAL DESCRIPTION AND PROPERTIES

Cuprous Sulfide ($Cu_2S_{1.01}$), P-type

Source:	Stanford Research Institute
Description:	Copper and sulfur (1% excess) cast in cylindrical form in graphite mold. Polycrystalline specimen cut to dimensions.
Dimensions:	3.050 cm x .510 cm x .510 cm
Heat Treatment:	Specimen annealed at about 400°C followed by slow cooling.

Cuprous Sulfide - General Properties
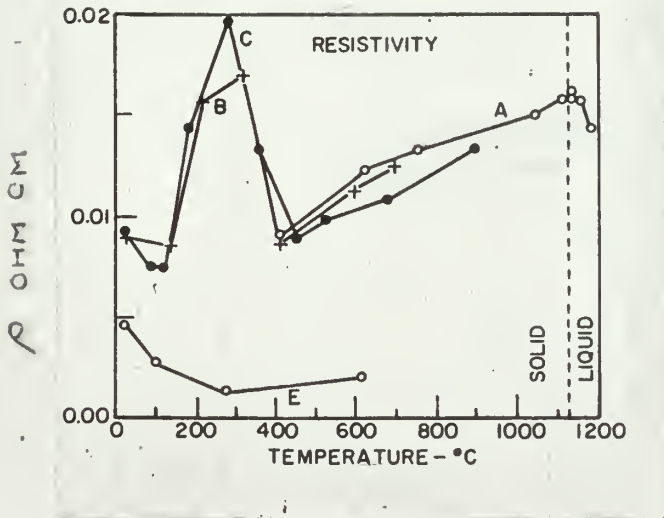
Note: Curve E for Ni doped specimen

Fig. 11 Resistivity Data, Cuprous Sulfide (about 1% excess sulfur) [2] .
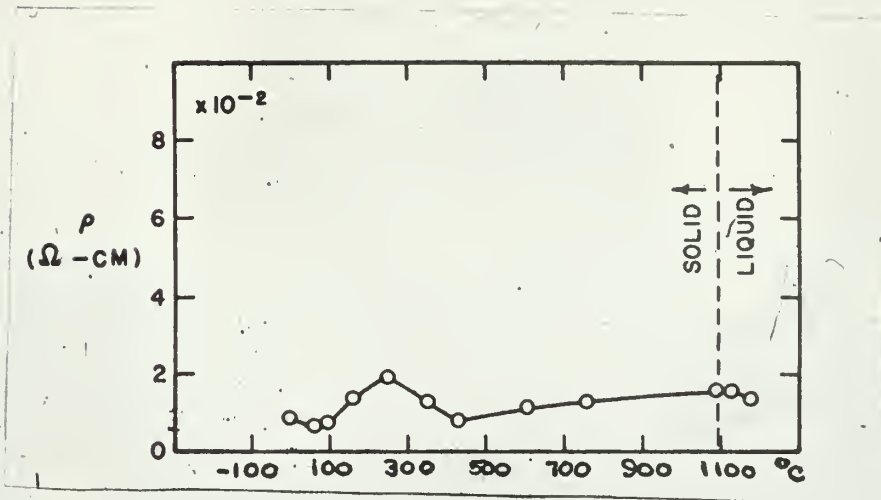
Fig. 12 Resistivity Data, Cuprous Sulfide (about 1% excess sulfur) [11] .
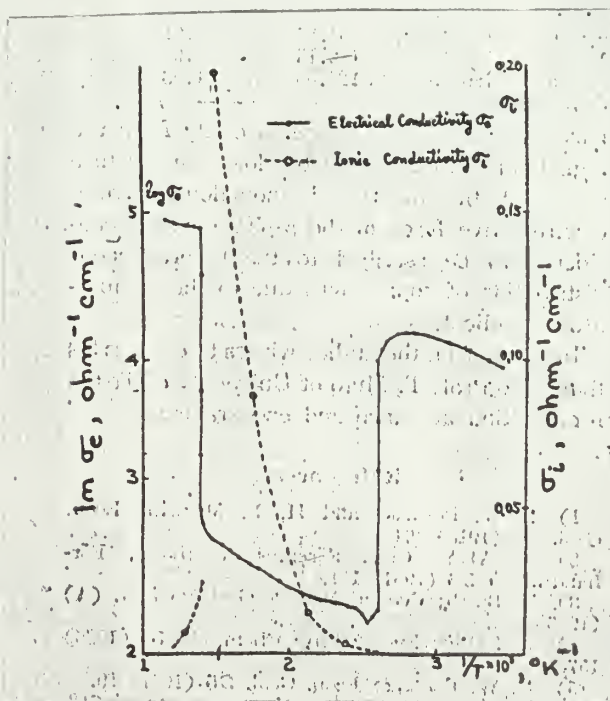
Fig. 13 Ionic and Electrical Conductivity, Cuprous Sulfide (stoichiometric) [4]
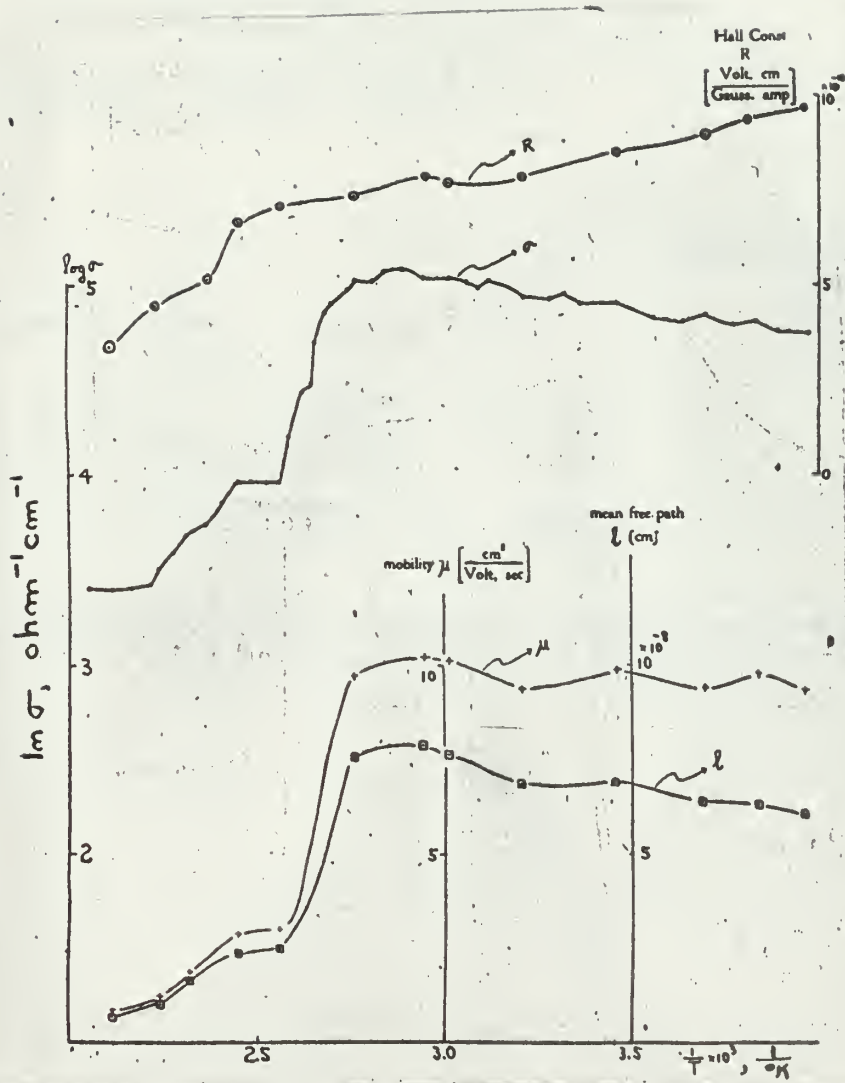
Fig. 14 Hall Constant, Electrical Conductivity, Mobility, and Mean Free Path Length, Cuprous Sulfide (0.2% excess sulfur) [5].

Bismuth Telluride (Bi_2Te_3), N-type

> Source: Merck and Company, Lot No. 50E-196E
>
> Description: Material furnished in cylindrical form.
>
> Crystal cut to dimensions.
>
> Dimensions: (Approximate) 3.0 cm x 0.50 cm x 0.50 cm with
>
> long dimension in direction of layers.
>
> Heat Treatment: None, preliminary to run.

Bismuth Telluride - General Properties
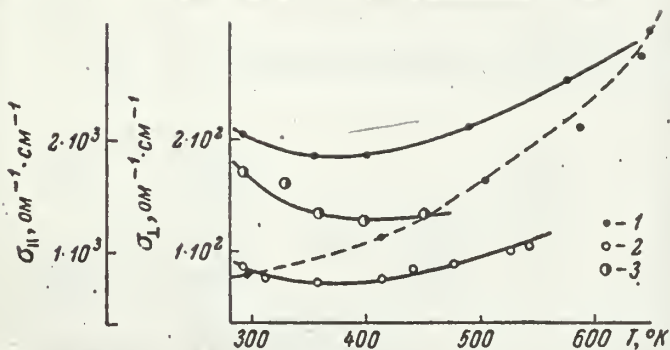
Note: Solid curves for outer scale, dashed curve for inner scale.

Fig. 15 Electrical Conductivity Parallel and Perpendicular to Layers, Bismuth Telluride (stoichiometric) [7]
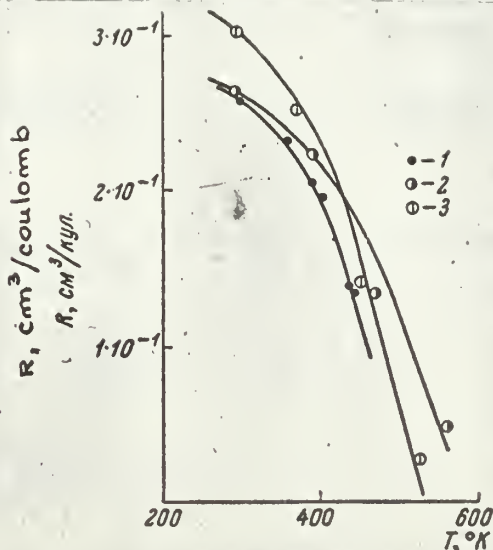
Fig. 16 Hall Coefficient, Bismuth Telluride (stoichiometric) [7]

APPENDIX II

Part A - Temperature Evaluation Technique

Thermal energy transfer for steady conditions is illustrated in

Fig. 17, assuming a uniform temperature at any given cross-section.
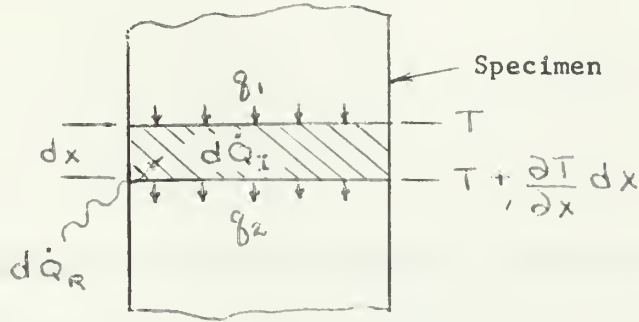
Fig. 17 Thermal Energy Transfer in Specimen Increment

$$-q_1 = kA \frac{dT}{dx}$$

$$-q_2 = kA \frac{dT}{dx} + kA \frac{\partial^2 T}{\partial x^2} dx$$

$$q_1 - q_2 = -kA \frac{\partial^2 T}{\partial x^2} dx$$

$$d\dot{Q}_I = \frac{I^2 \rho}{A} dx$$

$$d\dot{Q}_R = \frac{\dot{Q}_R}{L} = \dot{q}_R dx$$

(Assume ρ constant with x)

(Assume $\dot{q}_R$ constant with x)

Neglecting Thomson effect $\left(\dot{Q}_T = \gamma I \frac{\partial T}{\partial x} \right)$, for energy balance,

$$-kA \frac{\partial^2 T}{\partial x^2} dx - \frac{I^2 \rho}{A} dx - \dot{q}_R dx = 0$$

$$\frac{\partial^2 T}{\partial x^2} + \frac{I^2 \rho + \dot{q}_R A}{kA^2} = 0$$

39

Let
$$\frac{I^2 \rho + \dot{q}_R A}{k A^2} = a$$

Then
$$\frac{\partial^2 T}{\partial x^2} = -a$$

$$\frac{\partial T}{\partial x} = -ax + C_1$$

$$T = -\frac{ax^2}{2} + C_1 x + C_2$$

For boundary conditions, assuming symmetrical temperature distribution:

$$\frac{\partial T}{\partial x} = \frac{dT}{dx} = 0 \quad \text{at} \quad x = \frac{L}{2}$$

$$T = T_0 \quad \text{at} \quad x = 0, L$$

Then
$$C_1 = \frac{aL}{2}, \quad C_2 = T_0 \qquad \text{and}$$

$$T = -\frac{ax^2}{2} + \frac{aLx}{2} + T_0 = \frac{aL}{2}\left[x\left(1 - \frac{x}{L}\right)\right] + T_0$$

or
$$T - T_0 = C_1\left[x\left(1 - \frac{x}{L}\right)\right]$$

$$T_{\frac{L}{2}} - T_0 = C_1\left(\frac{L}{4}\right), \quad T_{\frac{L}{3}} - T_0 = C_1\left(\frac{2L}{9}\right)$$

Eliminating C_1,

$$T_{\frac{L}{3}} = \frac{8}{9} T_{\frac{L}{2}} + \frac{1}{9} T_0$$

For parabolic temperature distribution along the specimen as in Fig. 18,
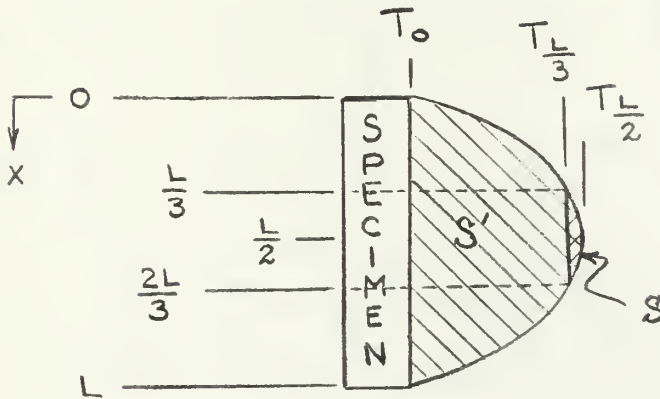
Fig. 18

Temperature Distribution Along Specimen

area $\quad S = \dfrac{4}{3}\left(\dfrac{L}{6}\right)\left(T_{\frac{L}{2}} - T_{\frac{L}{3}}\right) = \dfrac{2L}{9}\left(T_{\frac{L}{2}} - T_{\frac{L}{3}}\right)$

Then $\quad \bar{T}_S = \dfrac{2L}{9}\left(T_{\frac{L}{2}} - T_{\frac{L}{3}}\right) / \dfrac{L}{3} = \dfrac{2}{3}\left(T_{\frac{L}{2}} - T_{\frac{L}{3}}\right)$

But $\quad T_{\frac{L}{3}} = \dfrac{8}{9} T_{\frac{L}{2}} + \dfrac{1}{9} T_0$

and $\quad \bar{T}_{\frac{L}{3}\,\frac{2L}{3}} = T_{\frac{L}{3}} + \bar{T}_S = T_{\frac{L}{3}} + \dfrac{2}{3}\left(T_{\frac{L}{2}} - T_{\frac{L}{3}}\right)$

$\qquad\qquad = \dfrac{8}{9} T_{\frac{L}{2}} + \dfrac{1}{9} T_0 + \dfrac{2}{3}\left(T_{\frac{L}{2}} - \dfrac{8}{9} T_{\frac{L}{2}} - \dfrac{1}{9} T_0\right)$

$$\boxed{\; \bar{T}_{\frac{L}{3}\,\frac{2L}{3}} = \dfrac{26}{27} T_{\frac{L}{2}} + \dfrac{1}{27} T_0 \;}$$

This temperature derivation results in the average temperature based on a two-dimensional profile of an assumed parabolic distribution for the middle one-third section of the specimen, or between $x = \dfrac{L}{3}$ and $x = \dfrac{2L}{3}$

41

Area $\quad S' = \frac{4}{3}\left(\frac{L}{2}\right)\left(T_{\frac{L}{2}} - T_0\right) = \frac{2}{3}L\left(T_{\frac{L}{2}} - T_0\right)$

Then $\quad \bar{T}_{S'} = \frac{2}{3}L\left(T_{\frac{L}{2}} - T_0\right) \Big/ L = \frac{2}{3}\left(T_{\frac{L}{2}} - T_0\right)$

Hence $\quad \bar{T}_{0L} = T_0 + \bar{T}_{S'} = T_0 + \frac{2}{3}\left(T_{\frac{L}{2}} - T_0\right)$

$$\boxed{\bar{T}_{0L} = \frac{1}{3}T_0 + \frac{2}{3}T_{\frac{L}{2}}}$$

This derivation results in the average temperature for the entire specimen length from x = 0 to x = L.

Part B - Temperature correlations (platinum versus platinum plus 10% rhodium thermocouples)

Thermocouple number two was disengaged from the bottom electrode, repositioned to a midpoint position of the specimen, and shielded from the radiant heater. Thermal contact was maintained by the leaf spring action of a short length of tungsten wire, and contact checked by ohmmeter across thermocouple numbers one and two at each reading. At steady state conditions, T_0 and $T_{\frac{L}{2}}$ were recorded as follows:

T_0 (Thermocouple No. 1)		$T_{\frac{L}{2}}$ (Thermocouple No. 2)	
millivolts	°C	millivolts	°C
.090	16.0	.089	15.8
.183	31.8	.326	54.2
.388	63.6	.625	97.5

T_o (Thermocouple No. 1)		$T_{\frac{L}{2}}$ (Thermocouple No. 2)	
millivolts	°C	millivolts	°C
.515	82.1	.795	120.4
.564	89.0	.837	125.9
.693	106.9	1.051	153.2
.810	122.4	1.217	173.6
.901	134.1	1.360	190.9
1.028	150.4	1.465	203.4
1.068	155.4	1.540	212.2
1.205	172.2	1:746	236.1
1.420	198.1	2.098	275.9
1.600	219.2	2.395	308.7
1.775	239.4	2.635	334.7
1.920	255.9	2.790	351.2
2.135	280.0	3.070	381.0
2.495	319.6	3.413	416.9

An approximately linear correlation curve, T_o versus $T_{\frac{L}{2}}$, was plotted to a scale of .100 millivolts to the inch and is here represented in Fig. 19 on the page following, in greatly reduced scale for qualitative information.

Subsequent to the above correlation procedure, thermocouple number two was repositioned to the end of the specimen to enable check measurements of T_o and for ascertaining steady state conditions.

43

Temperature conversions from millivolts to degrees centigrade was
accomplished for specific levels associated with resistivity and
Hall voltage data, and determinations made in accordance with formulae
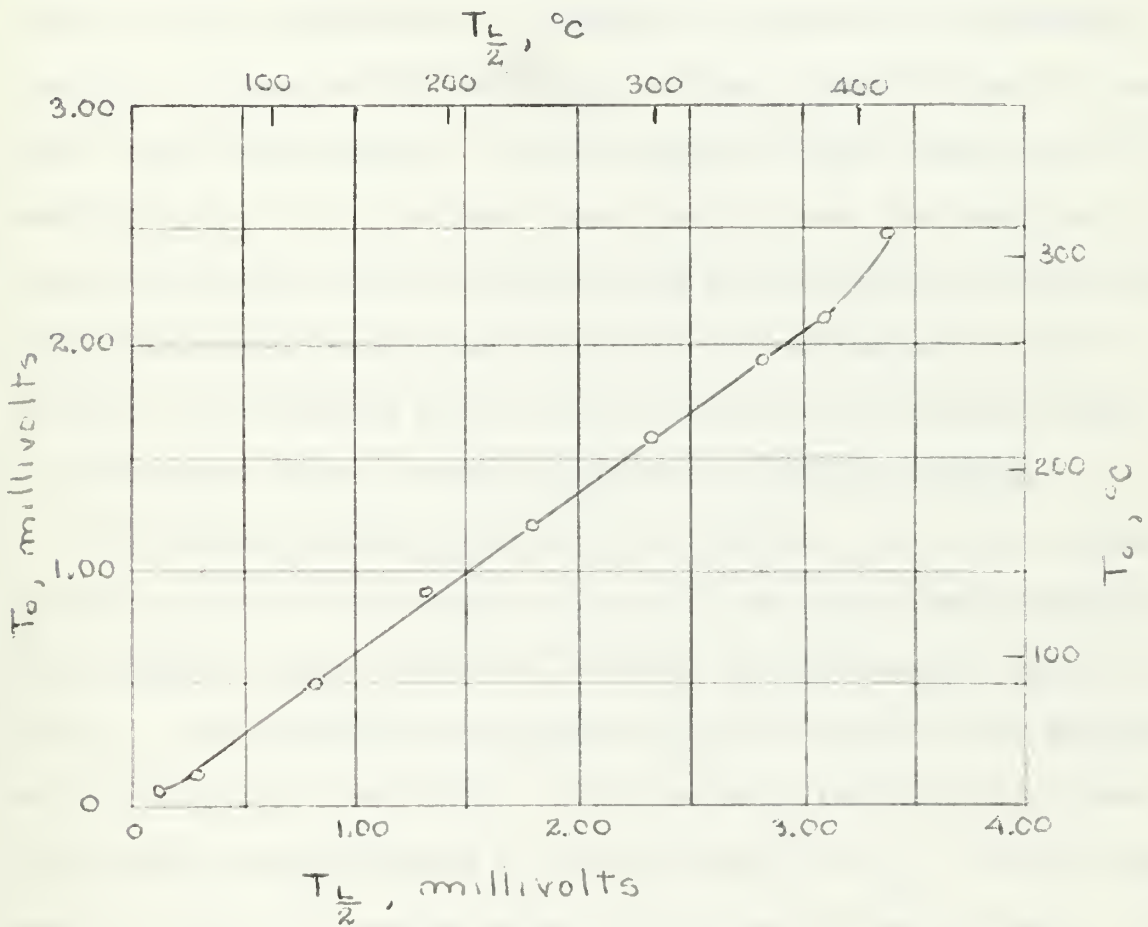developed in Part A of this Appendix.

Fig. 19 Thermocouple Correlation

APPENDIX III

EXPERIMENTAL ERROR

The experimental procedure entailed rapid consecutive readings
in order to (a) minimize the effect of Peltier heating and cooling and
(b) minimize the effect of Joule heating. As soon as steady-state thermal
conditions were established as recognized by constant end-thermocouple
readings, the specimen current circuit was then closed, followed by imme-
diate voltage measurements. With the potential probes located near the
central portion of the specimens, away from the ends, the disturbing in-
fluence on steady state of Peltier heating and cooling was not appreciable,
particularly with low specimen currents of 100 milliamperes or less.
Similarly, Joule heating did not greatly influence the presumed status
of steady state within the time required for necessary readings.

The assumed parabolic temperature distribution, as the best estimate,
did not account for the "shadows" imposed by the glass probe retainers or
the probes with their insulators. With the recorded boundary values, T_0
and $T_{\frac{L}{2}}$, the temperature distribution along the length of the specimen
has two reasonable limitations. On the one hand, the limit is a linear
distribution from the ends at T_0 to the midpoint at $T_{\frac{L}{2}}$. On the other
hand, the limit is a constant value at $T_{\frac{L}{2}}$ along the entire length. In
the former case, simple calculations based on averages of two-dimensional
temperature profiles show the largest difference of about 18 degrees at the
higher end of the temperature range, while, in the latter case, the maxi-
mum difference is about 33 degrees. These differences, of course, decrease
as $T_{\frac{L}{2}}$ approaches T_0 . It is logical to assume that the actual temperature

45

distribution did not approach either of these limits and, therefore, the true average temperatures were much more in accord with the tabulated values.

With temperature evaluations based upon a parabolic distribution, as best information in the absence of a complete temperature survey of each specimen, the equipment sensitivity of one microvolt produced a possible maximum reading error of one percent for a minimum temperature reading of about 100 microvolts and is relatively insignificant in this instance.

Further with regard to equipment sensitivity, the voltages reflecting average resistance were of such magnitudes as to produce a maximum reading error of about two percent, while the low Hall voltages were, at best, in 15 percent error increasing to an infinite value as the voltages approached the equipment sensitivity level.

The expediency of using a single calibration curve (Fig. 19, page 44), based upon measurements with the cuprous sulfide specimen in the holder, was adopted because of the similarity in the thermal conductivities of the two substances, bismuth telluride having thermal conductivities only slightly in excess by about 0.01 watts degrees^{-1} centimeters^{-1} at the lower end of the temperature range and increasing to about 0.04 watts degree^{-1} centimeter^{-1} at the higher end [3] .

Resistivity evaluations were directly related to the accuracy with which probe spacing was measured. Multiple averaged measurements produced the best dimensional data.

As a final consideration, some small transient effects caused a change in the thermoelectric power between the tungsten probes and the

46

specimens (being dissimilar materials), which added to and subtracted

from consecutive voltages, to produce minor error. The specimen

materials cannot be considered stable at elevated temperatures, parti-

cularly in an environment of strong magnetic and electric fields, as

evidenced simply by ionic motion. With a finite time required for conse-

cutive readings, some indeterminate thermocouple effects of a transient

nature in the probe-specimen circuit produced inaccuracies.

APPENDIX IV

CUPROUS SULFIDE - EXPERIMENTAL DATA

Thermocouple Readings E_1	E_2	Probes	EMF (IR Drop) V+	V-	Pressure p
millivolts			millivolts		microns
.120	.118	1 - 2	.751	-.750	5
.121	.120	3 - 4	.752	-.752	5
.185	.187	1 - 2	1.490	.059	8
.186	.188	3 - 4	1.481	.043	8
.241	.242	1 - 2	1.920	.580	9
.239	.239	3 - 4	1.908	.558	9
.302	.300	1 - 2	2.633	1.431	9
.305	.301	3 - 4	2.619	1.429	9
.364	.361	1 - 2	3.109	2.027	10
.370	.367	3 - 4	3.216	2.116	11
.420	.415	1 - 2	3.516	2.350	10
.421	.417	3 - 4	3.497	2.339	10
.560	.552	1 - 2	7.956	6.592	10
.562	.557	3 - 4	7.823	6.453	10
.627	.620	1 - 2	9.781	8.301	12
.629	.625	3 - 4	9.583	8.093	12
.733	.724	1 - 2	12.285	10.557	11
.735	.727	3 - 4	11.861	10.143	11
.809	.797	1 - 2	13.497	11.747	13
.811	.800	3 - 4	13.527	11.787	14
.980	.970	1 - 2	18.473	16.879	1.
.980	.975	3 - 4	17.980	16.394	12
1.163	1.151	1 - 2	22.003	20.623	12
1.159	1.157	3 - 4	22.778	21.386	11
1.323	1.311	1 - 2	27.320	26.178	10
1.320	1.313	3 - 4	27.920	26.800	10
1.453	1.440	1 - 2	30.267	29.335	9
1.460	1.455	3 - 4	28.384	27.438	10

CUPROUS SULFIDE - EXPERIMENTAL DATA

Thermocouple Readings E_1	E_2	Probes	EMF (IR Drop) $V+$	$V-$	Pressure p
millivolts			millivolts		microns
1.597	1.582	1 - 2	28.971	28.189	10
1.603	1.587	3 - 4	25.920	25.150	10
1.725	1.712	1 - 2	26.125	25.195	9
1.731	1.718	3 - 4	17.327	16.373	9
1.889	1.774	1 - 2	24.667	23.521	9
1.891	1.775	3 - 4	16.781	15.599	9
2.090	2.080	1 - 2	20.002	18.548	10
2.112	2.100	3 - 4	14.369	12.889	11
2.333	2.315	1 - 2	18.993	17.271	10
2.328	2.320	3 - 4	13.013	11.323	9
2.751	2.731	1 - 2	18.467	16.665	11
2.738	2.723	3 - 4	14.031	12.239	11
3.117	3.100	1 - 2	21.642	19.648	10
3.155	3.135	3 - 4	17.142	15.116	10

Note: Hall voltage $\leqslant |1|$ microvolt throughout entire run.

Current through specimen: 50 milliamperes

Magnetic field strength: 5700 gauss

Probe spacing:

    Probes 1 - 2   1.051 centimeters

    Probes 3 - 4   1.063 centimeters

Specimen cross-sectional area (mean):   .260 square centimeters

BISMUTH TELLURIDE - EXPERIMENTAL DATA

Thermocouple Readings E_1	E_2	Probes	EMF V+	V-	Pressure p	Hall Voltage V+	V-
millivolts			millivolts		microns	microvolts	
.121	.120	1 - 2	.583	-.562	10		
.122	.117	3 - 4	.578	-.561	10		
.120		1 - 3	.000	-.001			
	.120	1 - 3	.006	-.007	10	6	-6
.118	.120	2 - 4	.001	.000			
	.120	2 - 4	.006	-.004	10	5	-4
.446	.444	1 - 2	5.805	7.217	15		
.449	.447	3 - 4	4.155	5.554	15		
.450		1 - 3	1.719	1.755			
	.446	1 - 3	1.726	1.750	15	7	-5
.455		2 - 4	.073	.058			
	.451	2 - 4	.078	.053	15	5	-5
1.180	1.175	1 - 2	10.679	11.878	16		
1.184	1.181	3 - 4	5.310	6.496	16		
1.187		1 - 3	5.006	5.038			
	1.179	1 - 3	5.011	5.036	15	5	-2
1.190		2 - 4	.053	.042			
	1.181	2 - 4	.057	.039	15	4	-3
2.278	2.269	1 - 2	9.527	10.467	15		
2.285	2.286	3 - 4	5.435	6.340	15		
2.289		1 - 3	3.334	3.372			
	2.280	1 - 3	3.337	3.371	17	3	-1
2.295		2 - 4	.021	.019			
	2.289	2 - 4	.023	.019	17	2	0

BISMUTH TELLURIDE - EXPERIMENTAL DATA

Current through specimen: 100 milliamperes

Magnetic field strength: 5700 gauss

Probe spacing:

     Probes 1 - 2   1.03 centimeters

     Probes 3 - 4   0.99 centimeters

Specimen cross-sectional area: 0.25 square centimeters
                                       (approximate)

SAMPLE CALCULATIONS

CUPROUS SULFIDE SPECIMEN

Thermocouple Readings E_1 millivolts	E_2	Probes	EMF (IR Drop) V+ millivolts	V-	Hall Voltage V_H+ microvolts	V_H-
.302	.300	1 - 2	2.633	1.431		
.305	.301	3 - 4	2.619	1.429	< 1	< 1

Current through specimen: 50 milliamperes

Magnetic field strength: 5700 gauss

Probe spacing:

    Probes 1 - 2   1.051 centimeters

    Probes 3 - 4   1.063 centimeters

Specimen cross-sectional area (mean): 0.260 square centimeters

Specimen thickness, d: 0.510 centimeters

T_0 equals 0.302 millivolts, the arithmetic average of the four thermo-couple readings. Entering the T_0 versus $T_{\frac{1}{2}}$ correlation curve with this value, $T_{\frac{1}{2}}$ is established as 0.510 millivolts. From conversion tables for thermocouples in the case of platinum versus platinum plus ten percent rhodium:

0.302 millivolts equivalent to 50.5°C

0.510 millivolts equivalent to 81.4°C.

By formula developed in Appendix II,

$$\bar{T} = \frac{27}{27} T_{\frac{1}{2}} + \frac{1}{27} T_0 = 80°C \text{ or } 353°K$$

which is the average temperature of the specimen existing between probes.

$$V_{iR} = \frac{(v')-(v'')}{2} \tag{24}$$

For probes 1 - 2,

$$V_{iR} = \frac{(2.641 - 1.431)}{2}$$

For probes 3 - 4,

$$V_{iR} = \frac{(2.615 - 1.484)}{2}$$

and for an average value,

$$\overline{V}_{iR} = \frac{(.601 + .595)}{2}$$

$$\rho = \frac{VA}{L} = \frac{V_{iR}}{I} \cdot \frac{A}{L} \tag{1A}$$

$$\rho = \frac{(.598 \text{ mv})(.100 \text{ cm}^2)}{(50 \text{ ma})(1.057 \text{ cm})}$$

where L = 1.057 centimeters, an average value for probe spacing.

Hall's relation states

$$V_H = R_H \frac{IH}{d} \tag{5}$$

Then

$$R_H = \frac{V_H d}{IH} = \frac{(< 10^{-5} \text{ volt})(.)}{(.050 \text{ amp})()}$$

$$R_H < ..179 \times 10^{-5} \text{ volts} \dots$$

or converting from electrostatic units,

$$R_H < ..179 \quad \text{cm}^3/\text{coulomb}$$

for all temperatures within the range of investigation.

BISMUTH TELLURIDE SPECIMEN

Thermocouple Readings		Probes	EMF		Hall Voltage	
E_1	E_2		V+	V-	V_H+	V_H-
millivolts			millivolts		microvolts	
.450		1 - 3	1.719	1.755		
	.446	1 - 3	1.726	1.750	7	-5

Current through specimen: 100 milliamperes

Magnetic field strength: 5700 gauss

Specimen thickness, d: .50 centimeters

T_0 equals 0.448 millivolts, the average of the two thermocouple read-
ings during the measurements of Hall voltage between probes 1 and 3.
Entering the T_0 versus $T_{\bar{s}}$ correlation curve with this value, T
is established as 0.710 millivolts. From conversion tables for thermo-
couples in the case of platinum versus platinum plus ten percent rhodium

0.448 millivolt equivalent to 72.4°C

0.710 millivolts equivalent to 109.1°C

By formula developed in Appendix II,

$$\bar{T} = \frac{1}{3} T_{\bar{s}} + \frac{2}{3} T_0$$

which is the average temperature of the whole specimen during the
measurement of Hall voltage.

V_1 = V_{+} millivolts

V_2 = V_{+} + V_{-} millivolts

where V_1 is the measured voltage without the electromagnet energized, and V_2 is the measured voltage with the magnetic field of 5700 gauss. Then, subtracting,

$$V_H{}^+ = V_2 - V_1 = 7 \quad \text{microvolts}$$

Similarly,

$$V_H{}^- = V_2 - V_1 = -5 \quad \text{microvolts}$$

The average of the two absolute Hall voltages equals 6 microvolts.

$$R_H' = \frac{V_H d}{IH} = \frac{(6 \times 10^{-6} \text{volts})(.50 \text{ cm})}{(.100 \text{ amps})(5700 \text{ gauss})}$$

$$R_H = 0.53 \times 10^{-8} \text{ volts cm/amp gauss}$$

or converting from electrostatic units,

$$R_H = (-)\, 5.3 \times 10^{-1} \text{ cm}^3/\text{coulomb} \quad \text{at } 370°K$$

where R_H assumes a negative value for an N-type material.

Calculations for resistivity in the case of bismuth telluride were made for each set of probes, 1 - 2 and 3 - 4, and not averaged for tabulation.

APPENDIX VI

GLOSSARY OF GALVANOMAGNETIC, THERMOMAGNETIC, AND THERMAL EFFECTS

Ettinghausen Effect - a thermal gradient normal to a longitudinal electric current and a transverse magnetic field.

Ettinghausen-Nernst Effect - an electric field normal to the direction of a longitudinal heat current and a transverse magnetic field.

Hall Effect - an electric field normal to the direction of a longitudinal electric current and a transverse magnetic field.

Nernst Effect - a change in thermal gradient in the direction of an electric current in an applied magnetic field.

Righi-Leduc Effect - a thermal gradient normal to the direction of a longitudinal heat current and a transverse magnetic field.
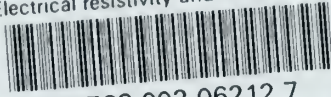
Peltier Effect - a change in temperature at the junction of two dissimilar materials through which an electric current passes.

Seebeck Effect - an EMF in an electric circuit with two junctions at different temperatures and of dissimilar materials.

Thomson Effect - the generation or absorption of heat in a material by the passage of an electric current along a temperature gradient.